2nd Micro and Nano Flows Conference
West London, UK, 1-2 September 2009

A way to visualise heat transfer in 3D unsteady flows

Michel F.M. Speetjens

* Corresponding author: Tel.: ++31 (0)40 2475428;
Email: m.f.m.speetjens @tue.nl

Energy Technology Laboratory, Mechanical Engineering Department, Eindhoven University of Technology, The Netherlands

Abstract Heat transfer in fluid flows traditionally is examined in terms of temperature field and heat-transfer coefficients. However, heat transfer may alternatively be considered as the transport of thermal energy by the total convective-conductive heat flux in a way analogous to the transport of fluid by the flow field. The paths followed by the total heat flux are the thermal counterpart to fluid trajectories and facilitate heat-transfer visualisation in a similar manner as flow visualisation. This has great potential for applications in which insight into the heat fluxes throughout the entire configuration is essential (e.g. cooling systems, heat exchangers). To date this concept has been restricted to 2D steady flows. The present study proposes its generalisation to 3D unsteady flows by representing heat transfer as the 3D unsteady motion of a virtual fluid subject to continuity. The heat-transfer visualisation is provided with a physical framework and demonstrated by way of representative examples. Furthermore, a fundamental analogy between fluid motion and heat transfer is addressed that may pave the way to future heat-transfer studies by well-established geometrical methods from laminar-mixing studies.

Keywords: Heat-Transfer Visualisation, Laminar Flows, Micro-Fluidics

1. Introduction

Industrial heat transfer problems may roughly be classified into two kinds of configurations. First, configurations in which the goal is rapid achievement of a uniform temperature field from a non-uniform initial state ("thermal homogenisation"). Second, configurations in which the goal is accomplishment and maintenance of high heat-transfer rates in certain directions. Thermal homogenisation is relevant for e.g. attainment of uniform product properties and processing conditions (polymers, glass, steel) and its key determinant is the temporal evolution of the temperature field towards its desired uniform state (see e.g. Lester et al., 2009). Sustained high heat-transfer rates are relevant for e.g. heat exchangers, conjugate heat transfer, thermofluids mixers and cooling applications and the key determinants here are the direction and intensity of heat fluxes (see e.g. Shah and Sekulic (2003). The present study concentrates on the latter kind of heat-transfer problems and then specifically under laminar flow conditions. This is motivated by the persistent relevance of viscous thermofluids (polymers, glass, steel) and, in particular, by the growing importance of compact applications due to continuous miniaturisation of heat-transfer and thermal-processing equipment (Sundén and Shah, 2007), the rapid development of micro-fluidics (Stone et al., 2004) and the rising thermal challenges in electronics cooling (Chu et al., 2004).

Heat transfer traditionally is examined in terms of convective heat-transfer coefficients at non-adiabatic walls as a function of the flow conditions (Shah and Sekulic, 2003). However, heat transfer may alternatively be considered as the transport of thermal energy by the *total* convective-conductive heat flux in a way analogous to the transport of fluid by the flow field. This concept has originally been introduced by Kimura and Bejan (1983) for 2D steady flows and has found application in a wide range of studies (a review is in Costa, 2006). Here the thermal trajectories are defined by a thermal streamfunction; a generalisation to generic 3D unsteady flows may lean on describing heat transfer as the "motion" of a "fluid" subject to continuity by the approach proposed in Speetjens (2008). This admits 3D heat-transfer visualisation by isolation of the thermal trajectories delineated by a "thermal velocity" in the same way as flow visualisation involves isolation of the fluid trajectories delineated by the fluid velocity.

The fluid-motion analogy is particularly suited for laminar flows, where flow and thermal paths are well-defined, and affords insight into the thermal

transport beyond that of conventional methods by disclosing heat fluxes throughout the *entire* domain of interest, that is, in all flow regions and solid walls instead of just on solid-fluid interfaces. Thus this ansatz has great potential for the thermal analysis of the (compact) heat-transfer problems that motivate this study. Though beyond the present scope, the fluid-motion analogy furthermore enables heat-transfer analysis by well-established geometrical methods from laminar-mixing studies (Speetjens et al., 2006, Ottino and Wiggins, 2004). Thus, apart from the "mere" visualisation of heat fluxes considered in the present study, heat-transfer visualisation offers promising new ways for analysis of laminar heat-transfer problems.

The present exposition elaborates the heat-transfer visualisation and its application for thermal analyses by way of examples. Considered are a 2D steady, 3D steady and a 2D unsteady system. Furthermore, an first step towards generic 3D unsteady systems is made. The discussion ends with conclusions and an outlook to future investigations.

2. Heat-transfer visualization: general

For incompressible fluids, the non-dimensional energy equation collapses on the form

$$\frac{\partial T}{\partial t} + \nabla \cdot \vec{Q} = 0\,, \quad \vec{Q} = T\vec{u} - \frac{1}{Pe}\nabla T\,, \qquad (1)$$

with $\vec{Q}$ the total physical heat flux due to combined convective and conductive heat transfer and Pe the well-known Péclet number, representing the ratio of convective to conductive heat transfer (Speetjens 2008). The temperature is defined such that T=0 corresponds with the minimum temperature in the domain of interest. The velocity field $\vec{u}$ is governed by the well-known continuity and momentum (Navier-Stokes) equations.

Flux $\vec{Q}$ in (1) delineates the thermal transport routes in an analogous way as the velocity $\vec{u}$ delineates the transport routes of fluid parcels. The paths followed by the total heat flux ("thermal trajectories") are the thermal counterpart to fluid trajectories and admit heat-transfer visualisation in a similar manner as flow visualisation. Furthermore, since $\vec{Q}$ is defined in flow and solid regions, heat-transfer visualisation is possible in the entire configuration. This has great potential for studies on thermal fluid-solid interaction and conjugate heat transfer, both cases of evident practical relevance. The heat-transfer visualisation is elaborated in the following by way of examples.

3. 2D Steady heat-transfer visualisation

3.1 Introduction

2D steady heat-transfer visualisation is demonstrated for a basic cooling problem. Considered is a square object (side length unity) with its bottom side maintained at a constant temperature *T=1* and exposed to a steady incompressible fluid flow with uniform inlet velocity *U=1* and at uniform inlet temperature *T=0*. Relevant parameters are *Pe*, as defined before, the fixed Reynolds number *Re=10* and the fixed ratio of thermal conductivities $\Lambda = \lambda / \lambda_o = 2$, with "o"' referring to the object. Only *Pe* is varied here. For the heat transfer in the object $\vec{Q} = -Pe^{-1}\nabla T$ and *Pe* is substituted by $Pe_o = Pe/\Lambda$ in (1). Numerical methods for resolution of the flow and temperature fields and the heat-transfer visualisation are furnished in Speetjens and van Steenhoven (2009).

3.2 Flow visualisation: fluid streamlines

2D steady flow via continuity implies a solenoidal mass flux $\vec{M} = \rho\vec{u}$, i.e. $\nabla \cdot \vec{M} = 0$, in turn, implying a stream function Ψ for the fluid motion, governed by

$$\frac{\partial \Psi}{\partial y} = M_x = \rho u_x\,, \quad \frac{\partial \Psi}{\partial x} = -M_y = -\rho u_y \qquad (2)$$

holding for arbitrary (non-constant) fluid density ρ. (Here $\rho = 1$; form (2) is retained to underscore the generality of the stream function.) The isopleths of Ψ coincide with the streamlines and thus visualise the flow field. Figure 1a gives the resulting streamline portrait, revealing the flow around the object and the formation of a recirculation zone in its wake.

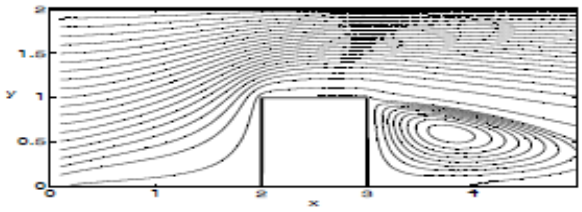

a) Streamline portrait

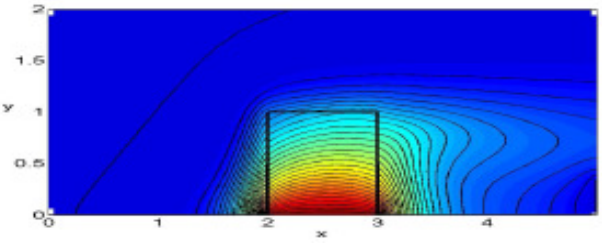

b) Temperature field

Fig. 1. 2D case study: (panel b: blue: *T=0*; red: *T=1*).

3.3 Heat-transfer visualisation: thermal streamlines

The present steady conditions reduce the energy equation (1) to $\nabla \cdot \vec{Q} = 0$, exposing the total heat flux $\vec{Q}$ as solenoidal. Thus the energy equation takes the same form as the steady-state continuity equation underlying (2). This mathematical equivalence naturally leads to the concept of a "thermal stream function" Ψ_T, which is governed by

$$\frac{\partial \Psi_T}{\partial y} = Q_x, \qquad \frac{\partial \Psi_T}{\partial x} = -Q_y,, \qquad (3)$$

as the thermal analogy to the stream function Ψ. The isopleths of Ψ_T delineate the sought-after thermal transport routes and are the thermal equivalent of the streamlines of the fluid flow (i.e. "thermal streamlines"). The thermal streamline portrait thus visualizes the heat transfer in essentially the same way as the streamline portrait visualises the fluid transport. This concept has originally been introduced by Kimura and Bejan (1983) and has found application in a wide range of studies (refer to Costa, 2006 for a review).

The equivalence between (2) and (3) implies a fundamental analogy between fluid and heat transport. First, it advances the total heat flux $\vec{Q}$ as the thermal counterpart to the mass flux $\vec{M}$. Second, it implies that (the isopleths of) Ψ and Ψ_T are subject to the same geometrical restrictions: the (thermal) streamlines cannot suddenly emerge or terminate; they must either be closed or connect with a boundary. This has fundamental ramifications for the transport properties in the sense that the (thermal) streamlines are organised into coherent structures that geometrically determine the fluid motion and heat transfer. For the fluid motion this manifests itself in the formation of a throughflow region, consisting of "channels" that connect inlet and outlet of the domain, and a recirculation zone (Figure 1a). For the heat transfer a similar organisation happens. This is demonstrated below.

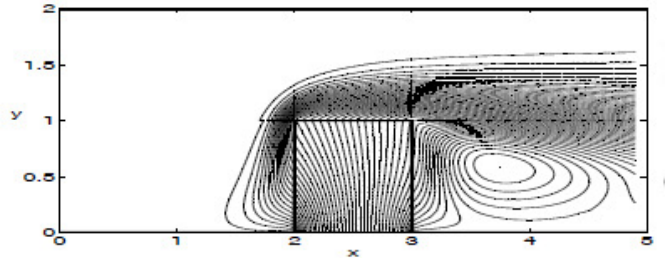

Fig. 2. 2D case study: thermal streamlines (Pe=50).

The temperature field is displayed in Figure 1b and its distribution clearly reflects the cooling of the object by the passing fluid. Figure 2 gives the corresponding thermal streamline portrait Ψ_T. The thermal streamlines bound, similar to its counterpart in the streamline portrait (Figure 1a), adjacent channels. These channels transport thermal energy in the same manner as stream tubes transport fluid and are the thermal equivalent to stream tubes ("heat conduits"). The fact that thermal streamlines must either be closed or connect with a boundary implies two kinds of heat conduits: (i) open heat conduits connected with boundaries; (ii) closed heat conduits. Both types are present in Figure 2 and their role in the heat transfer is considered below.

The open heat conduits inside the object facilitate the heat transfer from its hot bottom side through its interior towards the fluid-solid interface. Here the open heat conduits continue into the flow region and collectively form a "plume" that emerges from the perimeter of the object and rapidly aligns itself with the flow in downstream direction. This plume

constitutes the "thermal path" by which heat is removed from the object by the passing fluid. The thermal path is bend around a family of concentric closed heat conduits that collectively form a thermal recirculation zone ("thermal island"). The thermal island entraps and circulates thermal energy and, consequently, forms a thermally-isolated region. The blank region upstream of the thermal path has negligible heat flux ($\vec{Q} \approx \vec{0}$) and, consequently, renders Ψ_T undefined ("thermally-inactive region"). Thus heat-transfer visualisation exposes the several relevant regions of the heat-transfer problem and puts forth the thermal path as the only region actively involved in the cooling process of the object.

3.4 Thermal path: the role of convection

Heat transfer in the flow region has two asymptotic states: $Pe=0$ (purely-conductive heat transfer) and $Pe \to \infty$ (purely-convective heat transfer). The actual state sits between both asymptotic states for finite Pe and progresses from its conductive to its convective limit with rising Pe. This is demonstrated in Figure 3. For the conductive state (panel a) the thermal path occupies the entire flow region, signifying heat release into the entire domain and has two sections, separated by a separatrix emanating from the top wall of the object (not shown), the left and right of which transport heat to inlet and outlet, respectively, of the flow region. The separatrix propagates towards the lower-left corner of the object (panel b) with rising Pe until one thermal path connecting object with outlet forms (panel c). Furthermore, the thermal island emerges in the wake of the object and the thermal path becomes spatially more confined (panel d).

4. 3D Steady heat-transfer visualisation

4.1 Introduction

Here the 3D extension to the above cooling problem is considered. The configuration consists of a cubical object (side length unity) with its bottom side maintained at a constant temperature $T=1$ and exposed to a steady incompressible fluid flow with uniform inlet velocity $U=1$ and at uniform inlet temperature $T=0$. The system parameters are identical to those of the 2D counterpart. Numerical methods for resolution of the 3D flow and temperature fields and the 3D heat-transfer visualisation are furnished in Speetjens and van Steenhoven (2009).

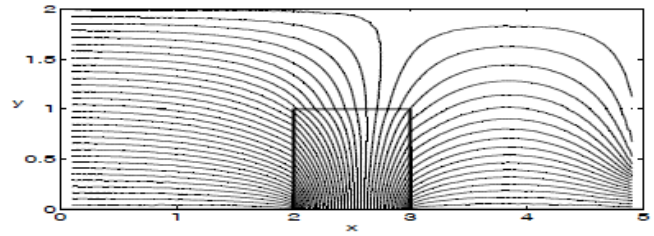

a) Pe=0

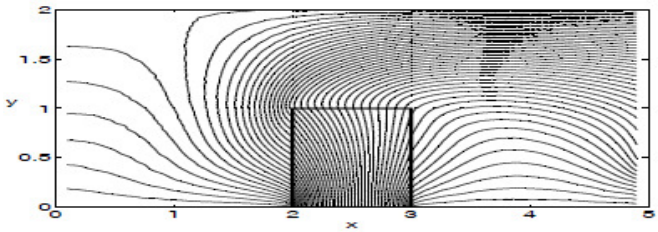

b) Pe=1

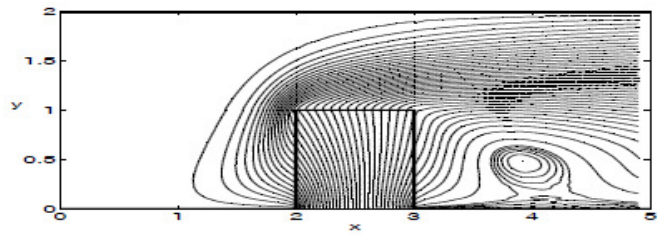

c) Pe=10

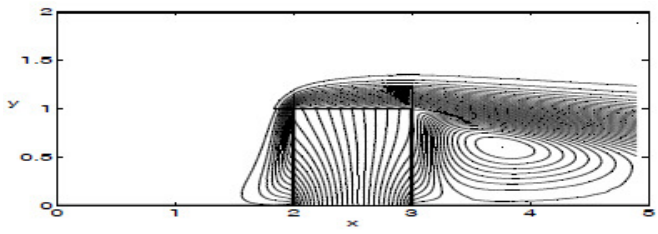

d) Pe=200

Fig. 3. Progression of the thermal streamline portrait with increasing Pe.

4.2 Flow visualisation: 3D streamlines

Essential difference with the 2D case is that in the 3D case streamfunctions no longer exists. Here the fluid streamlines $\underline{x}(t)$ are governed by

$$\frac{d\vec{x}}{dt} = \frac{\vec{M}}{\rho} = \vec{u}, \qquad \nabla \cdot \vec{M} = 0, \qquad (4)$$

with $\vec{M} = \rho\vec{u}$ the solenoidal mass flux as introduced before. Hence, the fluid streamlines coincide with the field lines of both $\vec{u}$ and $\vec{M}$. Note that (4) is a generalisation of the streamfunction relation (2).

Continuity imposes the same geometrical restrictions upon the 3D streamlines $\underline{x}(t)$ as found before for the 2D case: the streamlines cannot suddenly emerge or terminate; they must either be closed or connect with a boundary. This manifests itself, essentially similar to the 2D steady case, in the fact that continuity organises the streamlines into coherent structures, albeit of a greater variety and complexity due to the larger geometric freedom afforded by 3D conditions. These structures determine the topological make-up ("flow topology") of the web of fluid trajectories (Speetjensd at al., 2006, Malyuga et al., 2002). This flow topology is the generalisation of the 2D streamline portrait.

4.3 Heat-transfer visualisation: 3D thermal streamlines

The analogy between (thermal) stream functions Ψ and Ψ_T and mass and heat flux $\vec{M}$ and $\vec{Q}$ established before naturally leads to

$$\frac{d\vec{x}_T}{dt} = \frac{\vec{Q}}{T} = \vec{u}_T, \qquad \nabla \cdot \vec{Q} = 0, \qquad (5)$$

as thermal counterpart to (4) (Speetjens and van Steenhoven, 2009). The mathematical equivalence between (4) and (5) implies that heat transfer in essence is the "motion" of a "fluid" with "density" T propagating along thermal trajectories $\vec{x}_T$ delineated by a "thermal velocity" $\vec{u}_T$ subject to continuity. This, in turn, implies a "thermal topology" as thermal counterpart to the flow topology that is organised into the same kinds of coherent structures as the latter. The concept of a 3D thermal topology is exemplified below by the 3D thermal path originating from the 3D object.

4.4 Thermal path revisited

Figure 4 shows 3D thermal streamlines according to (5) emanating from the leading and trailing faces of the 3D object at *Pe=10*. These thermal streamlines, as in the 2D case (Figure 3), delineate the route along which heat is removed from the object by the passing flow and outline the 3D thermal path. Stronger convective heat transfer (increasing Pe) manifests itself similarly as before. First, increasing Pe causes the section of the thermal path connected with the inlet to vanish, meaning that beyond a certain Pe only heat exchange between object and outlet occurs. Second, increasing Pe leads to contraction of the thermal path around the object as well as contraction of its "tail," thus spatially confining the effective heat-transfer zone. This behaviour is in line with that of the 2D thermal path (Figure 3). The 3D thermal path -- and 3D thermal topology as a whole -- may exhibit greater topological complexity and in principle admits chaotic heat transfer, though. Further pursuit of this matter is beyond the present scope, however. Chaotic heat transfer is considered in the following section for 2D unsteady conditions, which in general is dynamically equivalent to that occurring in 3D steady systems (Speetjens, 2008).

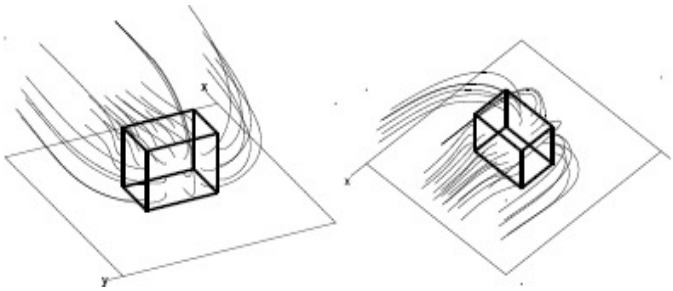

Fig. 4. 3D thermal path emanating from the hot object, visualised by 3D thermal streamlines originating from the leading and trailing faces of the object (Pe=10).

5. 2D Unsteady heat-transfer visualisation

5.1 Unsteady flow and heat-transfer visualisation

Relation (4) under unsteady conditions becomes

$$\frac{d\vec{x}}{dt} = \frac{\vec{M}}{\rho} = \vec{u}, \qquad \frac{\partial \rho}{\partial t} + \nabla \cdot \vec{M} = 0, \qquad (6)$$

and, via (1), naturally leads to

$$\frac{d\vec{x}_T}{dt} = \frac{\vec{Q}}{T} = \vec{u}_T, \qquad \frac{\partial T}{\partial t} + \nabla \cdot \vec{Q} = 0, \qquad (7)$$

as its thermal equivalent, meaning the physical analogy between fluid motion and heat transfer – and flow and thermal topologies – established above is upheld. The unsteady flow and thermal topologies, governed by (6) and (7), respectively, are illustrated hereafter for the heat transfer in a time-periodic flow (period time $\tau = 1$) set up by a horizontally-oscillating vortex pair inside a non-dimensional periodic channel (width W=1; height H=1/2) with hot bottom and cold top wall. The velocity field is given by the analytical expressions

$$\vec{u}(\vec{x},t) = \vec{u}(\vec{x},t+1) = \underline{\vec{u}}(\vec{x}_+(t)) + \underline{\vec{u}}(\vec{x}_-(t)), \qquad (8)$$

with $\vec{x}_{+/-}(t) = (x_0^{+/-} - \Delta x(t), 1/4)$ the positions of the two adjacent vortices ($x_0^- = 1/4$ and $x_0^+ = 3/4$) and $\Delta x(t) = \varepsilon \sin 2\pi t$ the oscillation at amplitude ε. The basic velocity reads $\underline{u}_x(\vec{x}) = \sin 2\pi x \cos 2\pi y$ and $\underline{u}_y(\vec{x}) = -\cos 2\pi x \sin 2\pi y$. System parameters are the Péclet number Pe (here fixed at Pe=10) and the amplitude ε. The employed numerical methods are detailed in Speetjens and van Steenhoven (2009).

5.2 Steady baseline

First the steady baseline ($\varepsilon = 0$) is considered for reference, shown in Figure 5. Panel a gives the streamline portrait, which consists entirely of islands that isolate and circulate fluid. The thermal streamline portrait (panel b) consists of a thermal path, connecting the channel walls and enabling fluid-wall heat exchange, and two adjacent thermal islands. This is, in addition to the cooling problem considered before, a further demonstration of the essential role of the thermal path in thermal fluid-structure interaction and, consequently, of its great practical importance.

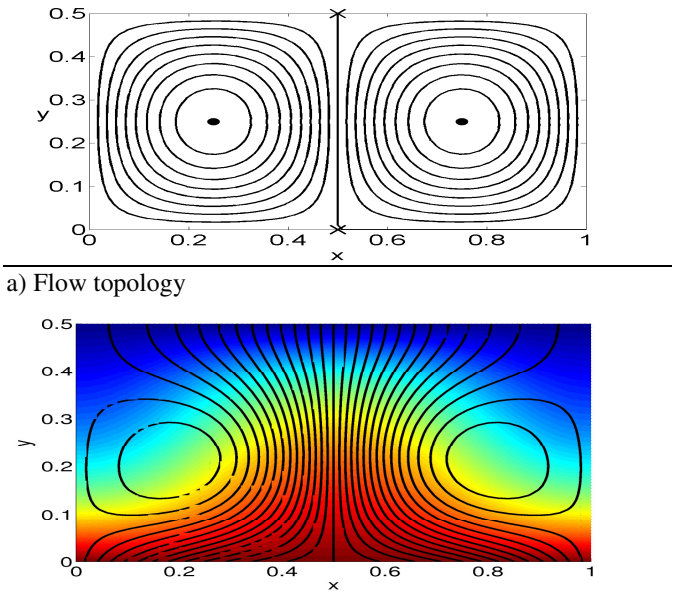

a) Flow topology

b) Thermal topology

Fig. 5. Flow and thermal topologies of a steady-vortex flow inside a periodic channel with hot bottom and cold top wall. Red/blue indicate highest/lowest temperature.

5.3 Flow visualisation: chaotic advection

The complexity of flow and thermal topologies expands under unsteady conditions. Here these conditions are attained by introduction of time-periodic horizontal oscillation of the vortex pair ($\varepsilon = 0.1$). The flow topology of time-periodic flows can be visualised by so-called Poincaré-sections, i.e. the subsequent positions of fluid parcels at the time levels $t \in [0, \tau, 2\tau, ...]$ following from stroboscopic "illumination" of the flow. The Poincaré-sections of fluid parcels released at "strategic" locations visualise the flow topology in a manner akin to the streamline portraits in steady flows. Figure 6a shows the Poincaré-sections (black dots) of fluid parcels released on the line $y = 1/4$, disclosing two kinds of coherent structures: (i) chaotic sea; (ii) islands embedded in the chaotic sea. The islands, similar to the steady case, isolate and circulate fluid; the chaotic sea is an essentially unsteady phenomenon. The red

and blue curves within the sea delineate the principal transport directions upon progression and regression in time, respectively, and are its underly-ing coherent structures. These curves (termed "manifolds") effec-uate chaotic advection (i.e. the complex motion of fluid parcels) and are key to the accomplishment of "efficient mixing" (Wiggins and Ottino, 2004). Vi-sualisation of the flow topology thus directly exposes the practically relevant poor and good mixing zones.

5.4 Heat-transfer visualisation: chaotic heat transfer

The thermal topology also admits chaotic seas, as visualised in Figure 6b by their corresponding manifolds ($\varepsilon = 0.1$). These manifolds, entirely analogous to their counterparts in the flow topology, effectuate chaotic heat transfer (efficient "mixing" of heat). Their attachment to the channel walls implies the formation of a chaotic thermal path in addition to the non-chaotic thermal path (of similar shape as shown in Figure 2b) occupying the region indicated by the stars. Thus unsteady effects result in the "chaotisation" of both internal heat transfer and thermal fluid-structure interaction. Thermal islands are absent here. The present approach pinpoints zones with chaotic advection and chaotic heat transfer and thus facilitates direct investigation of the connection between both transport phenomena. This is a topic of great practical relevance that remains ill-understood to date (Lester et al., 2009, Chang and Sen 1994, Mokrani et al., 1997). The present analysis, for instance, reveals that the chaotic regions in flow and thermal topologies do not coincide, implying that, contrary to common belief, chaotic heat transfer is not automatic with chaotic advection. Further analyses with the present approach revealed that, in the presence of chaotic advection, the chaotic-heat-transfer zones diminish (and eventually vanish) with increasing heat conduction (decreasing *Pe*) in favour of a non-chaotic thermal path (Speetjens, 2008, Speetjens and van Steenhoven, 2009). Such analyses are beyond the reach of conventional methods and reflect the great potential of the current ansatz for heat-transfer visualisation.

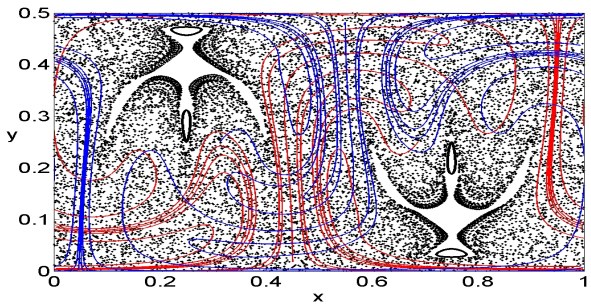

a) Flow topology

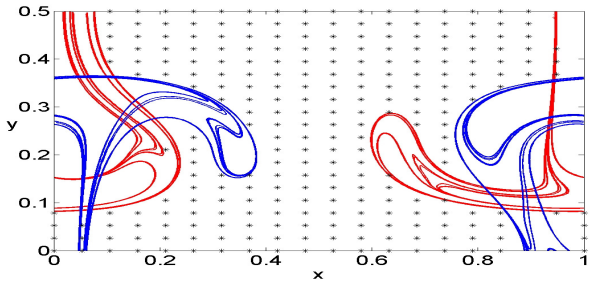

b) Thermal topology

Fig. 6. Flow and thermal topologies under time-periodic conditions shown in terms of Poincaré-sections. Blue and red curves indicate the principal transport directions in the chaotic zones; dots in panel a demonstrate chaotic advection; stars in panel b indicate region of regular thermal path.

6. Towards 3D unsteady heat-transfer visualisation

Heat-transfer visualisation in generic 3D unsteady systems is in essence similar to that demonstrated above for 2D time-periodic systems, since the thermal trajectories $\vec{x}_T$ remain governed by relations (7). However, 3D heat-transfer visualisation, despite resting on essentially the same concepts and methods, is complicated significantly on grounds of the far greater topological complexity 3D transport topologies may exhibit relative to those of 2D systems (Speetjens et al., 2006, Wiggins and Ottino, 2004, Malyuga et al., 2002) and, intimately related to that, the absence of a fully-developed theoretical framework. Moreover, the scenarios and mechanisms underlying the onset to 3D chaotic advection – and, inherently, chaotic heat transfer - are largely unexplored to date.

7. Conclusions

The study proposes an approach by which to visualise heat transfer in 3D unsteady laminar flows. This approach hinges on considering heat transfer as the transport of thermal energy by the *total* convective-conductive heat flux in a way analogous to fluid transport by the flow field. The paths followed by the total heat flux are the thermal counterpart to fluid trajectories and facilitate heat-transfer visualisation in a similar manner as flow visualisation. This has great potential for applications in which insight into the heat fluxes throughout the entire configuration is essential. To date this concept has been restricted to 2D steady flows. The present study proposes its generalisation to 3D unsteady flows by representing heat transfer as the 3D unsteady "motion" of a "fluid" subject to continuity. This affords insight into the thermal transport beyond that of conventional methods.

2D steady heat-transfer visualization centres on a "thermal stream function" that, analogous to the fluid stream function delineating the fluid streamlines, delineates the thermal transport routes ("thermal streamlines"). The thermal streamline portraits are, by virtue of continuity, organised into two kinds of coherent structures: thermal islands and thermal paths. Thermal islands consist of closed thermal streamlines and entrap and circulate heat. Thermal paths consist of open thermal streamlines attached to non-adiabatic walls and facilitate net heat exchange between these walls and the flow. Thermal paths thus are key to many practical heat-transfer problems.

The thermal topology in 3D steady systems is organised into similar coherent structures as in 2D systems, the most important of which again is the thermal path emanating from non-adiabatic walls. However, 3D systems may exhibit greater topological complexity and in principle admit chaotic advection and chaotic heat transfer. 2D unsteady systems are dynamically similar to 3D steady systems and also admit chaotic transport. The connection between chaotic advection and chaotic heat transfer is highly non-trivial, though. Thermal topologies in 3D unsteady systems, though admitting visualisation by essentially the same methods as their 2D counterparts, may exhibit an even greater topological complexity. Hence, their properties remain largely unexplored to date and are the subject of ongoing investigations.

The analogy between heat transfer and fluid motion facilitates analysis of heat-transfer problems by well-established geometrical methods from laminar mixing. This offers promising new ways for analysis of laminar heat-transfer problems. Studies to address these issues are in progress.

References

Lester, D. R., Rudman, M., Metcalfe, G., 2009. Low Reynolds number scalar transport enhancement in viscous and non-Newtonian fluids. Int. J. Heat Mass Transfer, 655.

Shah, R.K., Sekulic, D.P., 2003. Fundamentals of Heat Exchanger Design. Wiley, Chichester.

Sundén, B., Shah, R.K., 2007. Advances in Compact Heat Exchangers, Edwards. Philadelphia.

Stone, H. A., Stroock, A. D., Ajdari, A., 2004. Engineering flows in small devices: microfluidics toward a lab-on-a-chip. Ann. Rev. Fluid Mech. 36, 381.

Ottino, J. M. ,Wiggins, S., 2004. Introduction: mixing in micro-fluidics. Phil. Trans. R. Soc. Lond. A 362, 923.

Chu, R. C., Simons, R. E., Ellsworth, M. J., Schmidt, R. R., Cozzolino, V., 2004. Review of cooling technologies for computer products. IEEE Trans. Device Mat. Reliab. 4, 568.

Kimura, S. , Bejan, A., 1983. The heatline visualization of convective heat transfer. ASME J. Heat Transfer 105, 916.

Costa, V.A.F., 2006. Bejan's heatlines and masslines for convection visualization and analysis. ASME Appl. Mech. Rev. 59, 126.

Speetjens, M.F.M. , 2008. Topology of advective-diffusive scalar transport in laminar flows. Phys. Rev. E 77, 026309.

Speetjens, M., Metcalfe, G., Rudman, M., 2006. Topological mixing study of non-Newtonian duct flows. Phys. Fluids 18, 103103.

Wiggins, S., Ottino, J.M., 2004. Foundations of chaotic mixing. Phil. Trans. R. Soc. Lond. A 362, 937.

Malyuga, V. S., Meleshko, V. V., Speetjens, M. F. M., Clercx, H. J. H., van Heijst, G. J. F., 2002. Mixing in the Stokes flow in a cylindrical container. Proc. R. Soc. Lond. A 458, 1867.

Speetjens, M.F.M., van Steenhoven, A.A., 2009. A way to visualise laminar heat-transfer in 3D unsteady flows. Submitted to Int. J. Heat Mass Transfer.

Chang, H.-C., Sen, M., 1994. Application of chaotic advection to heat transfer. Chaos, Solitons & Fractals 4, 955.

Mokrani, A., Casterlain, C., Peerhossaini, H., 1997. The effects of chaotic advection on heat transfer. Int. J. Heat Mass Transfer 40, 3089.